Predicting Mechanical Properties of Metal Matrix Syntactic Foams Reinforced with Ceramic Spheres

J. B. Ferguson, J. A. Santa Maria, B. F. Schultz, P. K. Rohatgi

UWM Centers for Composites and Advanced Materials Manufacture University of Wisconsin-Milwaukee Materials Department CEAS, EMS 574 P.O. Box 784 Milwaukee, WI 53201 USA

Abstract

A model is presented that predicts peak stress, minimum stress, average stress, densification strain, and composite density in order to determine the energy absorption per unit volume and energy absorption per unit mass of metal matrix syntactic foams reinforced with hollow ceramic spheres subjected to unconstrained compression testing. Comparison of predictions to experimental data for Al-A206 and Al-A380 matrices of various heat treatments reinforced with Al_2O_3 spheres of various sizes, size ranges, and wall thickness to sphere diameter ratios show good agreement.

Introduction

Metal matrix syntactic foams (MMSF's) may be considered as underdeveloped when compared to open cell or closed cell foams. Though many studies have been conducted where selected properties of single matrix and reinforcement composition and reinforcement size combinations have been reported, little information is available on how to intelligently tailor these materials to obtain desired mechanical properties [1-19]. Moreover, these studies rarely report all of the mechanical properties of interest to engineers.

Critical review of the available literature is further complicated by the fact that there is not widespread agreement on the definitions of certain critical properties of MMSF's as they differ from conventional metal foams. For example, the definition of plateau stress (i.e. the single stress level at which a foam material absorbs a significant amount of strain before densification) is problematic in these materials as the stress varies significantly between the peak and densification. Densification strain is even more arbitrary as some studies report properties to fixed strains (for example 30% strain or 50% strain), while others report densification strain at such high strain that the stresses are much higher than the peak stress. Parts 1 and 2 of this series [20, 21] defined the plateau stress as the average stress between the strain at peak stress and the strain at densification. For consistency, the densification strain was defined as the strain at which the foam sustains a stress equal to the initial peak stress. This definition follows that used in metal foams- materials in which the peak stress and plateau stress are similar, where densification is considered to occur when the stress rises above the plateau stress (i.e. peak stress) [22]. This definition is also consistent with analyses of syntactic foams containing metallic hollow spheres [23]. Using these definitions the authors reported the effects of sphere dimensions, matrix composition and mechanical and physical properties on the foam's density, unconstrained compressive peak stress, plateau stress, densification strain, toughness (energy absorption per unit volume), and specific energy

Report Documentation Page

Form Approved
OMB No. 0704-0188

1. REPORT DATE	2. REPORT TYPE	3. DATES COVERED
13 AUG 2012	**Journal Article**	**13-08-2012 to 13-08-2012**

4. TITLE AND SUBTITLE
Predicting Mechanical Properties of Metal Matrix Syntactic Foams Reinforced with Ceramic Spheres

5a. CONTRACT NUMBER
w56hzv-08-c-0716

5b. GRANT NUMBER

5c. PROGRAM ELEMENT NUMBER

6. AUTHOR(S)
J. Ferguson; J. Santa Maria; B. Schultz; P. Rohatgi

5d. PROJECT NUMBER

5e. TASK NUMBER

5f. WORK UNIT NUMBER

7. PERFORMING ORGANIZATION NAME(S) AND ADDRESS(ES)
University of Wisconsin,Milwaukee Materials Department CEAS,Milwaukee,WI,53201

8. PERFORMING ORGANIZATION REPORT NUMBER
; #23253

9. SPONSORING/MONITORING AGENCY NAME(S) AND ADDRESS(ES)
U.S. Army TARDEC, 6501 E.11 Mile Rd, Warren, MI, 48397-5000

10. SPONSOR/MONITOR'S ACRONYM(S)
TARDEC

11. SPONSOR/MONITOR'S REPORT NUMBER(S)
#23253

12. DISTRIBUTION/AVAILABILITY STATEMENT
Approved for public release; distribution unlimited

13. SUPPLEMENTARY NOTES

14. ABSTRACT

A model is presented that predicts peak stress, minimum stress, average stress, densification strain, and composite density in order to determine the energy absorption per unit volume and energy absorption per unit mass of metal matrix syntactic foams reinforced with hollow ceramic spheres subjected to unconstrained compression testing. Comparison of predictions to experimental data for Al-A206 and Al-A380 matrices of various heat treatments reinforced with Al2O3 spheres of various sizes, size ranges, and wall thickness to sphere diameter ratios show good agreement.

15. SUBJECT TERMS

16. SECURITY CLASSIFICATION OF:			17. LIMITATION OF ABSTRACT	18. NUMBER OF PAGES	19a. NAME OF RESPONSIBLE PERSON
a. REPORT	b. ABSTRACT	c. THIS PAGE			
unclassified	**unclassified**	**unclassified**	**Same as Report (SAR)**	**15**	

absorption (i.e. energy absorption per unit mass). The data from these systematic studies is presented in Table 1 and Table 2.

There is a general lack of models to predict or even describe the properties of MMSFs. The properties relevant to the design of a syntactic foam system for energy absorption that should be targeted for modeling include the foam's density, densification strain, peak stress and average stress based on the material properties of the components as well as their relative concentration (i.e. volume fraction). From these parameters toughness and specific energy can be determined. Balch and Dunand [24] have modeled the Elastic Modulus in Al-7075/silica-mullite hollow spheres, but this is not useful in predicting the properties of interest listed above. Kiser et al. [12] extended a metal foam model to account for ceramic reinforcement to predict the compressive strength, σ_{com} (i.e. peak strength).

$$\sigma_{com} \cong 5\sigma_{y_m}\left[1 - V\%_s\left(1 - 2\frac{t}{D}\right)^3\right]^3 \quad (1)$$

Figure 1 presents the peak stress predicted by the above model compared to the experimental peak stress from the data shown in Table 1 and Table 2. The prediction of the Kiser et al. [12] model deviates significantly from the experimental data and thus does not accurately describe the peak stress of these MMSFs. The objective of this article is to provide models predicting the physical and mechanical properties of MMSFs relevant to the design of materials for energy absorption. The predictions of the models are compared to the experimental data of A380-Al_2O_3 and A206-Al_2O_3 reported previously and reproduced in Table 1 and Table 2.

Model

Foam Density:

The density of the foam can be estimated by a rule of mixtures relationship using the volume fraction and density of each component.

$$\rho_{sf} = V\%_m\rho_m + (1 - V\%_m)\rho_s \quad (2)$$

It will be assumed that the volume percent and area percent of the spheres (considered as solid spheres having a density corresponding to the bulk density of the hollow spheres) are equivalent.

$$V\%_s = A\%_s \quad (3)$$

Densification Strain:

To estimate the densification strain, ε_D, it is assumed that the unconstrained specimen is a cylinder of radius R undergoing constant volume deformation ($V_D = V_t$) only longitudinally and not laterally (i.e. no barreling: $R_D = R_o = R$) until all hollow reinforcements are crushed. Assuming the wall thickness of the hollow reinforcement is negligible, the strain to densification is approximately equal to the volume fraction of spheres as shown below.

$$\varepsilon_D = \frac{l_o - l_D}{l_o} = \frac{\pi R^2(l_o - l_D)}{\pi R^2 l_o} = \frac{V_{sf} - V_D}{V_{sf}} = \frac{V_d}{V_{sf}} \cong \frac{V_s}{V_{sf}} = V\%_s \quad (4)$$

Peak Stress:

Considering that for an unconstrained compression test a unit element of the foam is subjected to uni-axial compressive stress ($\sigma_1 = \sigma,\ \sigma_2 = \sigma_3 = 0$) the maximum shear stress will act at a 45° angle from the axis of applied stress and is equal to half the applied stress.

$$\tau = \sigma/2 \tag{5}$$

The shear stress is intensified in the sphere wall because the shear stress applied over the entire sphere cross-section must be supported by only the fraction of the cross-section containing the wall material. This intensification is greatest at the equatorial plane where the ratio of wall area to cross-sectional area, A_w/A_s, is the smallest.

$$\tau_w = \frac{\tau}{A_w/A_s} = \frac{\sigma/2}{A_w/A_s} \tag{6}$$

The diameter of the hollow space, d, is determined by the diameter of the sphere, D, and the thickness of the sphere wall, t.

$$d = D - 2t \tag{7}$$

The ratio A_w/A_s can then be described using the ratio of wall thickness to diameter, t/D.

$$\frac{A_w}{A_s} = \frac{\pi(D^2-d^2)/4}{\pi D^2/4} = 1 - \frac{d^2}{D^2} = 4\left[\frac{t}{D} - \left(\frac{t}{D}\right)^2\right] \tag{8}$$

Failure of the wall will occur when the shear stress reaches the fracture strength of the wall material.

$$\tau_{f_w} = \frac{\sigma_{fw}}{2} \tag{9}$$

However, this assumes a defect-free monolithic wall material, which is likely an unrealistic assumption given the variability exhibited by actual spheres as demonstrated in Figure 2.

Therefore, actual failure will occur at only a fraction, n, of the monolithic compressive fracture strength.

$$\tau'_{f_w} = n\frac{\sigma_{fw}}{2} \tag{10}$$

The applied stress (nominal stress) is not solely concentrated in the sphere and must be partitioned between the matrix and the reinforcement. Assuming that this partition depends on the area fractions of each component, failure of the foam occurs when the matrix yields and the sphere wall fractures.

$$\sigma_f = A\%_m\sigma_{y_m} + A\%_s\tau'_{f_w} = \frac{\sigma_p/2}{A_w/A_S} \tag{11}$$

It is then possible to determine the expression for the peak stress of the foam.

$$\sigma_p = \left[2A\%_m\sigma_{y_m} + (1 - A\%_m)n\sigma_{f_w}\right]\left(\frac{A_w}{A_S}\right) \tag{12}$$

As the above equation tends to zero as wall thickness approaches zero, it ignores any strength of the matrix material. Therefore, strictly speaking, this treatment is only applicable if the overall behavior is dominated by the properties of the sphere. If the strength of the sphere is negligible, the behavior of the material would clearly be governed by the matrix strength adjusted for porosity. The critical sphere area ratio, $(A_w/A_s)^*$, below which peak stress is determined by the matrix and above which peak stress is dominated by the sphere occurs when the peak stress equals the porosity adjusted matrix yield strength.

$$A\%_m\sigma_{y_m} = \left[2A\%_m\sigma_{y_m} + (1 - A\%_m)n\sigma_{f_w}\right]\left(\frac{A_w}{A_s}\right)^* \quad (13)$$

$$\left(\frac{A_w}{A_s}\right)^* = \frac{A\%_m\sigma_{y_m}}{2A\%_m\sigma_{y_m} + (1-A\%_m)n\sigma_{f_w}} \quad (14)$$

All of the foams considered here are above this critical limit.

Minimum Stress, Average Stress, and Toughness:

Figure 3 shows the two types of post-peak deformation behavior in syntactic foams: Type I, where the matrix yields and spheres fracture simultaneously and Type II, where the spheres fracture before the matrix yields. Type I shows a gradual drop from peak stress followed by some dwelling at stresses near the minimum until approximately half the densification strain is reached and then rises monotonically until the peak stress is attained at the densification strain. Type II shows a more immediate drop to the minimum stress and an approximately linear rise to the peak stress at the densification strain.

The minimum stress developed in the material has been empirically determined to follow a rule of mixtures type of relationship taking into consideration the properties of the sphere and the intensification of the stress in the wall material at the equatorial plane.

$$\sigma_{min} = A\%_m\sigma_A + (1 - A\%_m)\frac{n\sigma_{f_w}}{2}\left(\frac{A_w}{A_s}\right) \quad (15)$$

The parameter σ_A depends on the type of behavior of the foam and can be predicted given the peak stress and the yield stress of the matrix. For Type I $\sigma_p \geq \sigma_{y_m}$ and $\sigma_A = \sigma_{UTS_m}$. For Type II $\sigma_p < \sigma_{y_m}$ and $\sigma_A = \sigma_{y_m}$ (in this case, $\sigma_{min} = \sigma_p/2$).

The average stress can be predicted assuming an ideal description of each type of foam behavior. In this case, the elastic strain of the material is considered negligible and the total plastic strain is assumed to be approximately equal to the densification strain.

$$\sigma_{pl_I} = \left[\sigma_{min}\frac{\varepsilon_D}{2} + \frac{\sigma_{min}+\sigma_p}{2}\left(\frac{\varepsilon_D}{2}\right)\right]/\varepsilon_D = \frac{(\sigma_p+3\sigma_{min})}{4} \quad (16)$$

$$\sigma_{pl_{II}} = \left[\frac{\sigma_{min}+\sigma_p}{2}\varepsilon_D\right]/\varepsilon_D = \frac{\sigma_{min}+\sigma_p}{2} \quad (17)$$

The Toughness, E/V, as defined as the area under the stress strain curve (i.e. Energy/Volume of Material) is easily calculated given the average stress and the densification strain. This again assumes that the plastic strain to densification is equivalent to the densification strain.

$$E/V = \sigma_{pl}\varepsilon_D \quad (18)$$

Specific energy absorption, E/m, is then the Toughness divided by the foam density.

$$E/m = \frac{E/V}{\rho_{sf}} \quad (19)$$

Comparison to Experimental Data

Table 2 lists the material properties of each matrix condition used in synthesizing the syntactic foams by Santa-Maria et al. [20,21]. For the as-cast materials, the yield stress and UTS are expected to be sensitive to grain size, which is difficult to determine in these materials. Therefore, these values should only be considered approximate. The precipitation hardened Al-A206 T4 and T7 materials are expected to show less sensitivity to grain size in yield stress and roughly similar UTS values [26].

For the alumina spheres used in this study, it is assumed that σ_{f_w}=2100 MPa and $n \cong 0.5$ and from the data of Figure 4, the sphere bulk density appears to be linearly dependent on average sphere diameter.

Given the experimentally determined properties listed in Table 1 and Table 2, the theoretical properties have been predicted. Figure 5 to Figure 11 compare experimental and theoretical values.

Figure 5 shows excellent agreement between the experimental data for peak stress and those predicted by the model. Figure 6 and Figure 7 agree very well at lower stress levels, but slightly under-predict experimental values at the higher stresses. This is due to infiltration of the spheres, where the matrix is no longer composed of only metal, but is a composite of metal reinforced by filled ceramic spheres. Therefore, the use of alloy properties, rather than the higher (but unknown) composite property predicts minimum and average stresses that are slightly lower than what was attained in the material.

The densification strain comparison of Figure 8 shows considerable scatter, though this is symmetrical about the line describing equivalent experimental and predicted values. The scatter in this data causes scatter in the Toughness data, but Figure 9 still shows decent agreement between the predicted and experimental data.

Figure 10 shows that the rule of mixtures prediction of density is in rough agreement between the largest and smallest spheres, but over-predicts by as much as 30% at intermediate sizes. Given the number of assumptions inherent in the predicted value including: $A\%_m$ being equivalent to $V\%_m$, no effect of infiltration of broken spheres, no shrinkage or gas porosity in the matrix, sphere properties correlate with average sphere properties), this is perhaps not surprising. Figure 11 shows the specific energy absorption predictions with the scatter resulting from the scatter in the density data.

Conclusion

The model presented is able to predict peak stress, minimum stress, average stress, densification strain, and composite density in order to determine the Toughness and specific energy absorption of metal matrix syntactic foams reinforced with hollow ceramic spheres subjected to unconstrained compressive stresses. The model takes into consideration the two types of post-peak deformation behavior of syntactic foams; I) namely matrix yield simultaneous with sphere fracture and II) sphere fracture before

additional matrix yielding. Comparison of predictions to experimental data for Al-A206 and Al-A380 matrices of various heat treatments reinforced with Al_2O_3 spheres of various sizes, size ranges, and wall thickness to sphere diameter ratios show excellent agreement for peak stress and good agreement for minimum and average stresses. Scatter in densification strain and foam density lead to scatter in the toughness and specific energy absorption, though the model still predicts the correct general trend.

Acknowledgement

This research was supported by the U.S. Army-TARDEC through TACOM R&D Contract# W56HZV-08-C-0716. Disclaimer: Reference herein to any specific commercial company, product, process, or service by trade name, trademark, manufacturer, or otherwise, does not necessarily constitute or imply its endorsement, recommendation, or favoring by the United States Government or the Department of the Army (DoA). The opinions of the authors expressed herein do not necessarily state or reflect those of the United States Government or the DoA, and shall not be used for advertising or product endorsement purposes.

Nomenclature:

σ_{com} = compressive strength (i.e. peak strength)	$A\%_s$ = area percentage of hollow spheres
σ_{y_m} = yield strength of matrix	$A\%_m$ = area percentage of matrix
σ_{UTS_m} = tensile strength of matrix	$V\%_s$ = volume percentage of hollow spheres
σ = applied stress	$V\%_m$ = volume percentage of matrix
σ_f = fracture stress of foam	t = wall thickness of hollow sphere
σ_{f_w} = fracture strength of hollow sphere wall	D = outside diameter of hollow sphere
σ_p = peak stress of syntactic foam	$\overline{D}$ = average diameter of hollow sphere
σ_{min} = minima stress of syntactic foam	d = inside diameter of hollow sphere
σ_A = adjusted strength of matrix	V = volume of syntactic foam
σ_{pl} = average (plateau) stress	m = mass of syntactic foam
$\sigma_{pl\ I}$ = average (plateau) stress Type I foam	R = radius of compression specimen
$\sigma_{pl\ II}$ = average (plateau) stress Type II foam	R_o = original specimen radius
τ = shear stress	l_o = original specimen length
τ_w = maximum shear stress at wall of hollow sphere	V_t = volume of solid in syntactic foam
τ_{f_w} = Ideal hollow sphere wall shear stress at failure	R_D = radius of fully dense specimen
τ'_{f_w} = Actual hollow sphere wall shear stress at failure	l_D = length of fully dense specimen
ϵ_D = strain at densification	V_D = volume of fully dense specimen
ϵ_p = strain at peak stress	V_{sf} = volume of bulk syntactic foam
E = energy	V_d = volume of pores
ρ_{sf} = bulk density of the foam	V_s = volume of hollow spheres
ρ_m= density of the matrix	A_w = Area of hollow sphere wall
ρ_s = bulk density of the hollow spheres	A_s = Area of hollow sphere (including pore)
	n= sphere defect correction factor

References

1. Balch DK, O'Dwyer JG, Davis GR, Cady CM, Gray III GT, Dunand DC. Mater Sci Eng A 2005; 391:408.
2. Dou ZY, Jiang LT, Wu GH, Zhang Q, Xiu ZY, Chen GQ. Scr Mater 2007; 57:945.
3. Wu GH, Dou ZY, Sun DL, Jiang LT, Ding BS, He BF. Scr Mater 2007; 56:221.
4. Zhang Q, Lee PD, Singh R, Wu G, Lindley TC. Acta Mater 2009; 57:3003.
5. Rohatgi PK, Kim JK, Gupta N, Alaraj S, Daoud A. Composites Part A 2006; 37:430.
6. Zhao Y, Tao X, Xue X. In Processing, Properties and Performance of Composite Materials, ed. Materials Science and Technology, Pittsburgh, PA, 2008, p.2607.
7. Tao XF, Zhang LP, Zhao YY. Mater Des 2009; 30:2732.
8. Tao XF, Zhao YY. Scr Mater 2009; 61:461.
9. Zhang LP, Zhao YY. J Compos Mater 2007; 41:2105.
10. Daoud A. J Alloys Compd. 2009; 487:618.
11. Drury WJ, Rickles SA, Sanders Jr TH, Cochran JK. In Light-Weight Alloys for Aerospace Applications, ed. Loe EW, Chia EH, Kim NJ. The Minerals, Metals and Materials Society, Warrendale, PA, 1989, p. 311.
12. Kiser M, He MY, Zok FW. Acta Mater 1999; 47:2685.
13. Mondal DP, Majumder JD, Jha N, Badkul A, Das S, Patel A, Gupta G. Mater Des 2012; 34:82
14. Orbulov IN, Dobránszky J. Period Polytech, Mech Eng 2008; 52:35.
15. Orbulov IN, Ginsztler J. Composites, Part A 2012; 43:553.
16. Palmer RA, Gao K, Doan TM, Green L, Cavallaro G. Mater Sci Eng A 2007; 464:85.
17. Rabiei A, Vendra LJ. Mater Lett 2009; 63:533.
18. Neville BP, Rabiei A. Mater Des 2008; 29:388.
19. Castro G, Nutt SR. Mater Sci Eng A 2012; 535:274.
20. Santa Maria J, Schultz BF, Ferguson JB, Gupta N, Rohatgi PK. TBA 2012; ##:## [380]
21. Santa Maria J, Schultz BF, Ferguson JB, Rohatgi PK. TBA 2012 [A206]
22. Ashby MF, Evans AG, Fleck NA, Gibson LJ, Hutchinson JW, Wadley HNG. Metal Foams, a Design Guide, Woburn, MA: Butterworth-Heinemann; 1998, p. 42-46.
23. Vesenjak M, Fiedler F, Ren Z, Ochsner A. Multifunctional Metallic Hollow Sphere Structures, ed. Ochsner A, Augustin C. Springer, Berlin, Germany, 2009, p. 65.
24. Balch DK, Dunand DC. Acta Mater 2006; 54:1501.
25. Santa Maria J. Master Thesis, University of Wisconsin Milwaukee, Milwaukee; 2012.
26. Talamantes-Silva M, Rodríguez A, Talamantes-Silva J, Valtierra S, Colás R. Metall Mater Trans B 2008; 39:911
27. J.G. Kaufman and E.L. Rooy., "Aluminum Alloy Castings: Properties, Processes, and Applications", American Foundry Society, 2004, pg. 94.
28. Properties and selection--nonferrous alloys and pure metals, Volume 9, Issue 2. ASM International, 1990, pg. 144.
29. Metals Handbook, Vol.2 - Properties and Selection: Nonferrous Alloys and Special-Purpose Materials, ASM International 10th Ed. 1990.

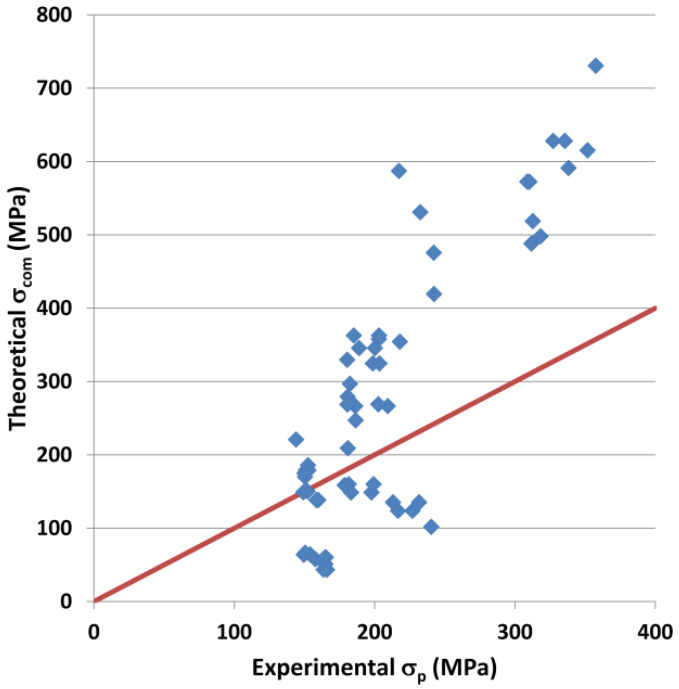

Figure 1 Prediction of Peak Stress using the Model of Kiser et al. [12]

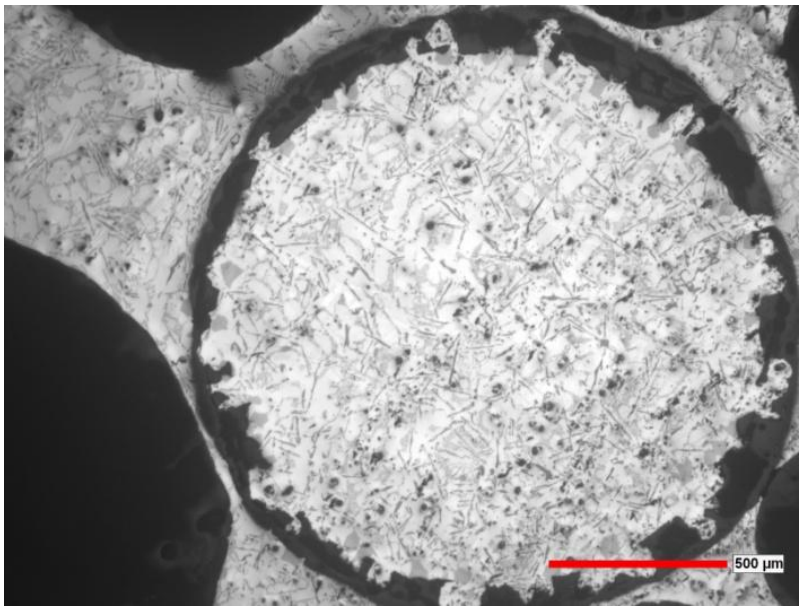

Figure 2 Al_2O_3 Sphere Infiltrated with Al-A380 Showing the Variability in Sphere Wall Thickness [25]

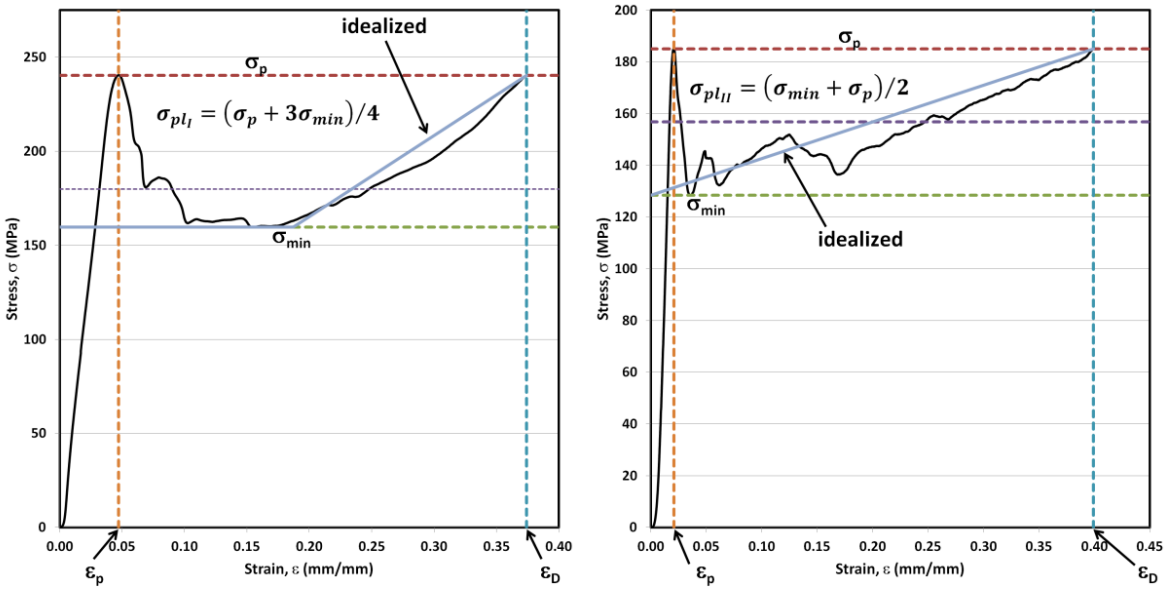

Figure 3 Typical Stress Strain Curve for Type I (left) and Type II (right) Foam Behavior [20,21]

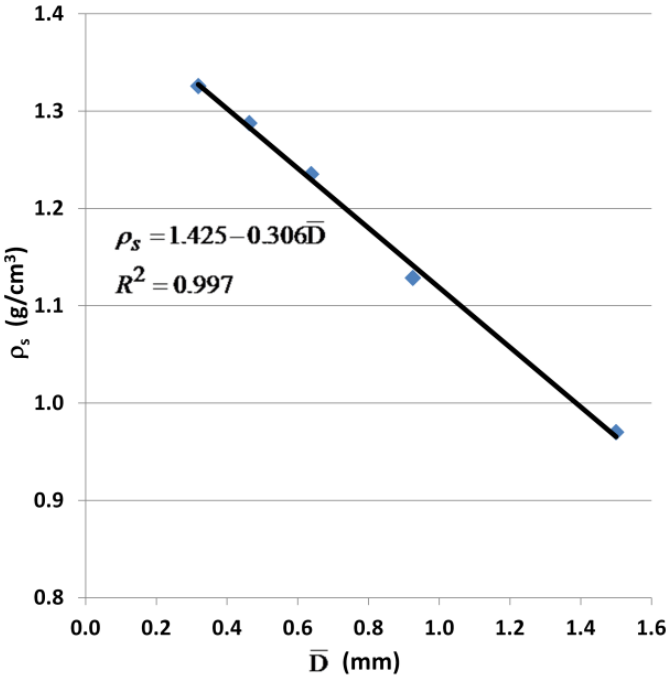

Figure 4 Dependence of Al_2O_3 Sphere Bulk Density on Average Sphere Diameter [data from 25]

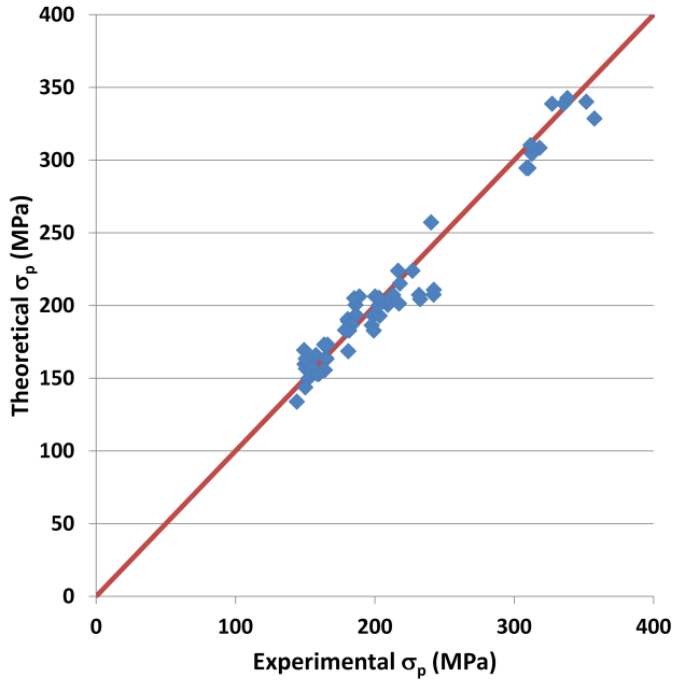

Figure 5 Comparison of Predicted Peak Stress to Experimentally Determined Peak Stress

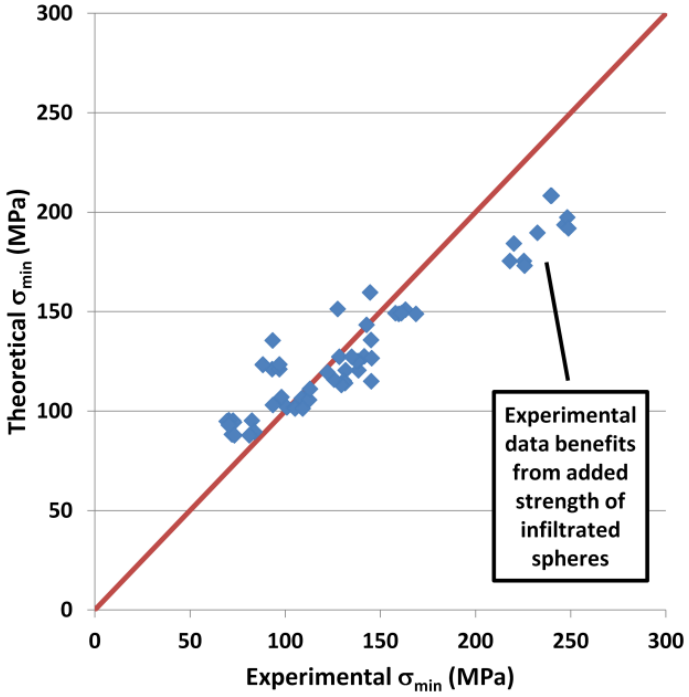

Figure 6 Comparison of Predicted Minimum Stress to Experimentally Determined Minimum Stress

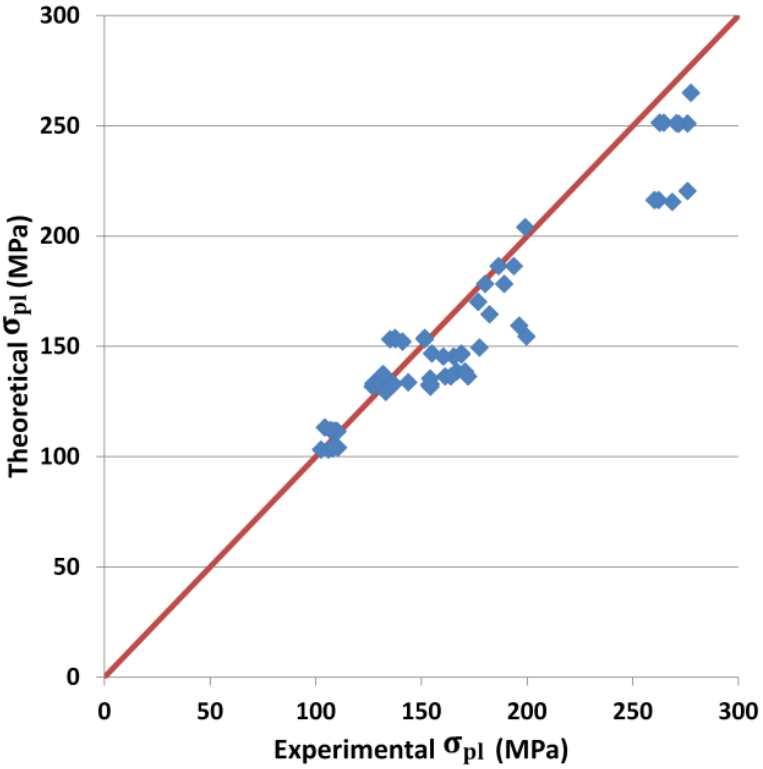

Figure 7 Comparison of Predicted Average Stress to Experimentally Determined Average Stress

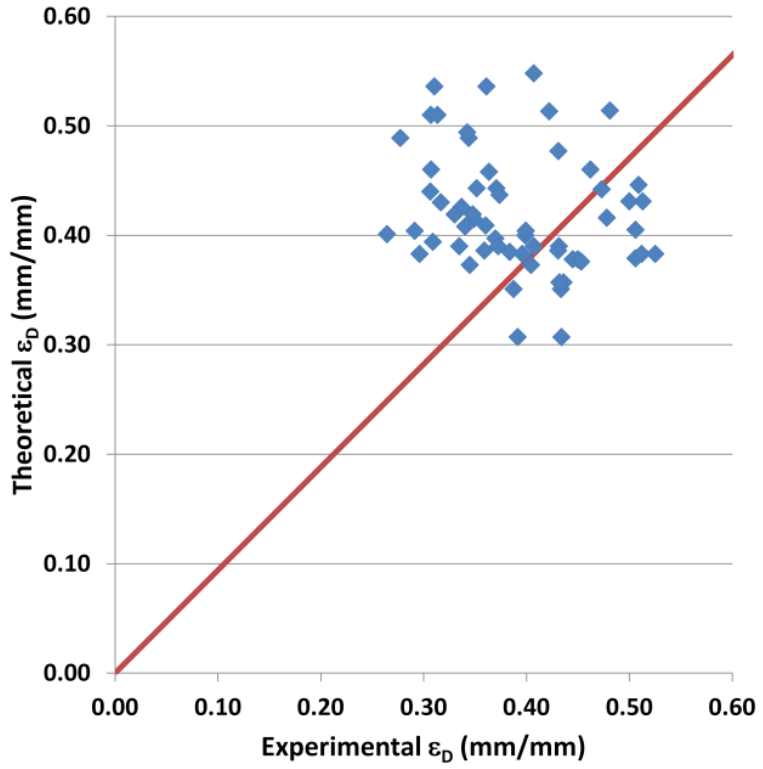

Figure 8 Comparison of Predicted Densification Strain to Experimentally Determined Densification Strain

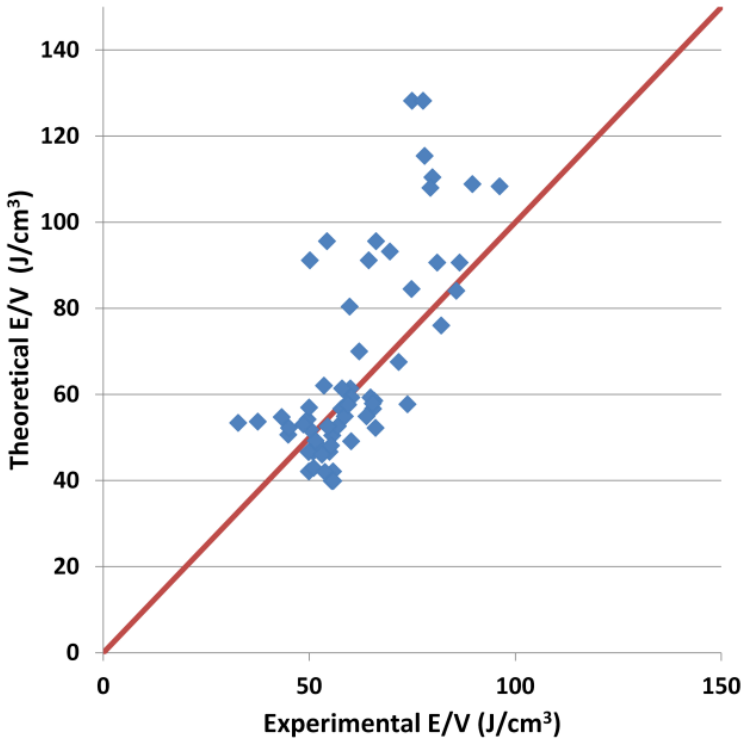

Figure 9 Comparison of Predicted Toughness to Experimentally Determined Toughness

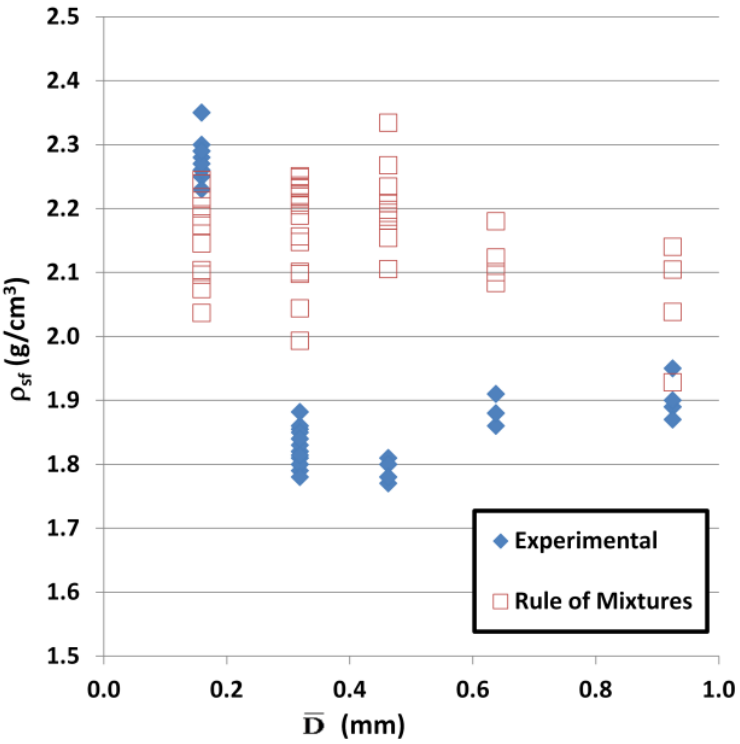

Figure 10 Comparison of Predicted Density to Experimentally Determined Density

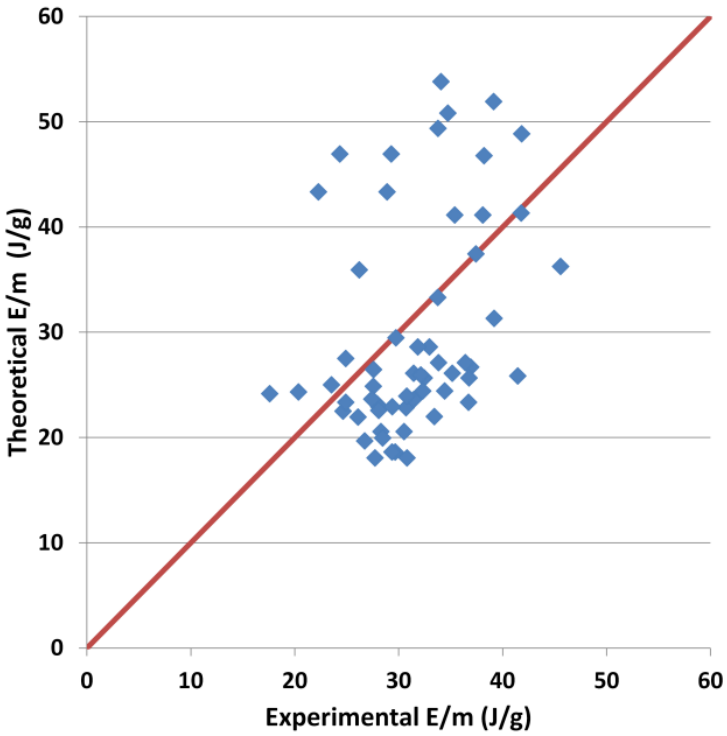

Figure 11 Comparison of Predicted Specific Energy Absorption to Experimentally Determined Specific Energy Absorption

Table 1 Experimental Results of Unconstrained Compression Testing of Al-A206/Al2O3 Syntactic Foams (Note: highlighted results treated as Type II behavior)

Cond.	Size (mm)	$\bar{D}$ (mm)	t/D	A_w/A_s	$A\%_m$ (%)	ρ_{sf} (g/cm^3)	ε_d	σ_p (MPa)	σ_{min} (MPa)	σ_{pl} (MPa)	E/V (J/cm^3)	E/m (J/g)
As-cast	0.106-0.212	0.159	0.105	0.377	39.4	2.28	0.31	240	163	199	59.7	26.2
					48.9	2.25	0.28	217	160	187	50.1	22.3
					48.9	2.23	0.34	227	169	194	64.4	28.9
					53.6	2.26	0.36	232	158	189	66.2	29.3
					53.6	2.23	0.31	213	161	180	54.3	24.3
	0.212-0.425	0.319	0.063	0.236	38.5	1.80	0.38	165	111	134	50.2	27.9
					40.4	1.84	0.29	154	111	131	37.5	20.4
					40.1	1.86	0.26	149	109	127	32.7	17.6
					41.5	1.84	0.35	150	98	127	43.3	23.5
					37.3	1.82	0.34	158	112	133	44.8	24.6
	0.425-0.500	0.463	0.060	0.227	35.1	1.80	0.39	165	101	137	50.9	28.3
					35.1	1.80	0.43	164	105	130	54.9	30.5
					39.0	1.81	0.43	164	94	133	55.6	30.7
					30.7	1.81	0.43	166	105	132	55.7	30.8
					30.7	1.80	0.39	164	109	132	49.9	27.7
T4	0.106-0.212	0.159	0.105	0.377	44.0	2.30	0.31	318	247	276	79.9	34.7
					51.0	2.35	0.31	310	239	263	74.9	31.9
					51.0	2.35	0.31	309	240	265	77.6	33.0
					46.0	2.29	0.31	313	248	272	78.0	34.1
					43.0	2.35	0.32	312	249	271	79.4	33.8
	0.212-0.425	0.319	0.063	0.236	44.3	1.82	0.37	199	138	167	60.0	32.9
					44.3	1.82	0.35	203	132	171	58.0	31.8
					38.3	1.81	0.30	186	145	161	45.1	24.9
					38.3	1.80	0.40	209	131	172	66.1	36.7
					38.6	1.81	0.36	202	131	164	56.9	31.4
	0.425-0.500	0.463	0.060	0.227	40.8	1.80	0.34	181	131	154	49.6	27.6
					39.7	1.77	0.37	180	130	154	54.5	30.8
					42.6	1.81	0.34	182	126	144	49.9	27.6
					45.8	1.80	0.36	180	122	154	53.5	29.7
					37.3	1.80	0.40	186	113	154	60.2	33.4
T7	0.106-0.212	0.159	0.105	0.377	40.9	2.30	0.36	352	232	278	96.2	41.8
					41.9	2.27	0.35	335	218	262	86.5	38.1
					41.9	2.29	0.33	327	225	260	81.0	35.4
					49.4	2.29	0.34	358	220	276	89.6	39.1
					39.0	2.29	0.33	338	226	269	85.7	37.4
	0.212-0.425	0.319	0.063	0.236	51.3	1.79	0.42	232	128	182	74.8	41.8
					47.7	1.80	0.43	242	143	196	82.0	45.6
					38.6	1.78	0.43	218	141	177	73.8	41.5
					54.8	1.82	0.41	217	145	177	69.5	38.2
					43.7	1.83	0.37	242	145	200	71.7	39.2
	0.425-0.500	0.463	0.060	0.227	40.0	1.78	0.40	203	145	169	65.7	36.9
					39.0	1.78	0.41	200	138	165	65.4	36.8
					39.0	1.78	0.37	189	138	160	57.8	32.5
					40.4	1.78	0.40	185	128	155	60.2	33.8
					40.4	1.78	0.40	203	135	169	64.8	36.4

Table 2 Experimental Results of Unconstrained Compression Testing of as-cast Al-A380/Al_2O_3 Syntactic Foams (Note: highlighted results treated as Type II behavior)

Size (mm)	$\bar{D}$ (mm)	t/D	A_w/A_s	$A\%_m$ (%)	ρ_{sf} (g/cm^3)	ε_d	σ_p (MPa)	σ_{min} (MPa)	σ_{pl} (MPa)	E/V (J/cm^3)	E/m (J/g)
0.212-0.425	0.319	0.063	0.236	35.7							
				35.7	1.81	0.43	183	97	138	58.6	32.3
				37.8	1.86	0.45	199	97	152	65.4	35.1
				37.8	1.88	0.45	182	88	135	59.1	31.4
				37.6	1.85	0.45	179	88	138	59.4	32.1
				46.0	1.84	0.46	181	93	141	62.1	33.7
0.425-0.85	0.638	0.058	0.219	43.1	1.86	0.50	151	73	109	52.2	28.1
				43.1	1.88	0.51	153	83	110	55.2	29.4
				37.9	1.91	0.51	149	73	104	51.0	26.7
				44.2	1.88	0.47	152	70	110	51.5	27.4
				41.6	1.91	0.48	150	69	107	49.8	26.1
0.85-1	0.925	0.052	0.199	40.5	1.89	0.51	152	72	108	53.8	28.5
				51.4	1.95	0.48	144	70	102	48.6	24.9
				44.6	1.89	0.51	150	84	106	53.1	28.1
				38.3	1.87	0.51	160	81	111	55.5	29.7
				38.3	1.90	0.53	159	73	109	55.8	29.4

Table 3 Matrix Properties

Matrix Condition	σ_{y_m} (MPa)	σ_{UTS_m} (MPa)	ρ_m (g/cm^3) [29]
Al-A206 As-Cast (estimated)	60	200	2.80
Al-A206 T4 [27]	262	428	
Al-A206 T7 [27]	345	435	
Al-A380 As-Cast [28]	160	324	2.76